Transient development of Zeeman electromagnetically induced transparency during propagation of Raman–Ramsey pulses through Rb buffer gas cell

2015 J. Phys. B: At. Mol. Opt. Phys. 48 045501

(http://iopscience.iop.org/0953-4075/48/4/045501)

J. Phys. B: At. Mol. Opt. Phys. **48** (2015) 045501 (11pp) doi:10.1088/0953-4075/48/4/045501

Transient development of Zeeman electromagnetically induced transparency during propagation of Raman–Ramsey pulses through Rb buffer gas cell

S N Nikolić, M Radonjić, N M Lučić, A J Krmpot and B M Jelenković

Institute of Physics, University of Belgrade, Pregrevica 118, 11080 Belgrade, Serbia

E-mail: stankon@ipb.ac.rs

Received 7 November 2014
Accepted for publication 18 December 2014
Published 30 January 2015

Abstract

We investigate, experimentally and theoretically, time development of Zeeman electromagnetically induced transparency (EIT) during propagation of two time separated polarization laser pulses, preparatory and probe, through Rb vapour. The pulses were produced by modifying laser intensity and degree of elliptical polarization. The frequency of the single laser beam is locked to the hyperfine $F_g = 2 \rightarrow F_e = 1$ transition of the D_1 line in ^{87}Rb. Transients in the intensity of σ^- component of the transmitted light are measured or calculated at different values of the external magnetic field, during both preparatory and probe pulse. Zeeman EIT resonances at particular time instants of the pulse propagation are reconstructed by appropriate sampling of the transients. We observe how laser intensity, Ramsey sequence and the Rb cell temperature affect the time dependence of EIT line shapes, amplitudes and linewidths. We show that at early times of the probe pulse propagation, several Ramsey fringes are present in EIT resonances, while at later moments a single narrow peak prevails. Time development of EIT amplitudes are determined by the transmitted intensity of the σ^- component during the pulse propagation.

Keywords: electromagnetically induced transparency, Ramsey effect, rubidium

(Some figures may appear in colour only in the online journal)

1. Introduction

Electromagnetically induced transparency (EIT) [1–3] is a quantum interference phenomenon which is manifestated as a narrow spectral resonance observed in transmitted laser light through otherwise opaque vapour of, typically, alkali metals. EIT is attained when two light fields couple two atomic ground levels to a common excited level (so-called Λ-scheme). Within the spectral bandwidth of the EIT there is a strong dispersion of the index of refraction, resulting in a slow light and storage of light phenomena in EIT medium [4, 5]. EIT is demonstrated as a coherent technique for controlling the propagation of classical light pulses and other nonlinear optics applications [4]. A review of EIT in various atomic schemes is given in [6].

Studies of pulse propagation through EIT medium is a mature field. Measurements of transient fluorescence [7], of transient gains of the probe pulse [8], and of non-resonant (for both preparation and probe beams) transients [9] were done. Also, transient effects in adiabatic [10] and non-adiabatic [11] regimes, depending if the rise time of the pulse is slow or fast compared to the Rabi period and relaxation times, were analyzed. Transients of transmission of the probe pulse were studied for cases when the pump beam is turned off [9] or on [11], when the probe itself is turned on, and when pump and probe fields are suddenly detuned from the resonance [8, 12]. Detailed theoretical investigation of EIT and features of the space-time dependent probe field in Λ-, V-, and cascade-type schemes are presented in [13]. The same authors performed a time-dependent analysis of the four-wave mixing process

(FWM) in a double-Λ system, showing that generated FWM field can acquire ultraslow group velocity [14].

It was shown that the pulse strength of the laser, the pulse switching rate, and the magnetic field determine the rate at which transmitted pulse reaches a new steady state. These parameters also determine transient behavior of the probe transmission with or without free induction decay [15]. Stepwise Raman detuning of circularly polarized pump and probe beams resulted in the oscillatory behavior of the transient signal, with the period of oscillations depending on the Raman detuning [16]. Dependence of decay rates of the amplitudes of the signal oscillations on the cell temperature and laser power was studied in [12]. Behavior of transmission of lasers inducing Zeeman EIT, when magnetic field is suddenly turned off and on, was studied both experimentally and theoretically [17]. Transients in coherent population trapping (CPT) can be also induced by ac magnetic field as calculated in [18, 19]. Transient response of an EIT media to a phase-modulated pump was examined in [20].

Propagation of a probe pulse through EIT medium is closely related to temporal evolution of EIT resonance. However, the transient development of EIT was much less studied than transmission of the laser pulse. In [21], the build up of EIT was observed after sudden two-photon detuning from EIT. It was found that the Zeeman EIT width decreases inversely with the interaction time and approaches an asymptotic value determined by the preparatory laser intensity [21].

Various models of transient effects were developed to predict, or to explain, the propagation of the laser pulse through EIT medium. Typically, analytical solutions of equations for density matrix describing a three-state model is used [15]. In [22] the authors compared transients for the dressed-atom and bare-atom pictures. The calculations of temporal evolution of EIT were also studied [23]. The transient response of atomic system was calculated when the laser is suddenly turned on in the presence of external magnetic field [24].

The Ramsey method of separated oscillatory fields [25] was applied to alkali atoms contained in the glass cell in order to narrow resonance linewidth. Application of two or more successive laser pulses leads to the appearance of high contrast and narrow (~100 Hz) CPT and EIT fringes [26–30]. Calculations have also shown that quantum interference, driven by two identical pulses, results in Ramsey-like fringes [31]. Two-photon free-induction decay in a three-level Λ system used to obtain EIT was reported in [32]. Ramsey interference effect appears after pulsed excitation, with fringes observed as time-domain oscillations in the transmission amplitude of a long attenuated query pulse [33]. Transient of Raman–Ramsey fringes (RRF) and EIT have been measured in sodium vapour in the hyperfine Λ system [34]. Ramsey fringes induced by Zeeman coherence in various Rb cells for both spatially and temporally separated laser fields were reported in [35]. Ramsey-like measurements of Zeeman decoherence that determine the dumping rate of such oscillations are presented in [36]. One application of Ramsey interference is frequency selective magnetometer based on light-pulse atom interferometry, as described in [37]. Implementation of a compact atomic clock based on Ramsey–CPT interference is proposed in [38].

This work extends previous studies of laser pulse propagation through EIT medium by observing transient development of Zeeman EIT during the pulse propagation. Experimentally and theoretically, we monitor intensity of the σ^- component during propagation of two time separated elliptically polarized laser pulses. The laser is locked to the D_1 line of ^{87}Rb. Zeeman EIT curves are reconstructed from transients of σ^- intensity at different external magnetic fields. We investigate transient behavior of the EIT line shapes, amplitudes and linewidths from the moments when laser pulses enter the Rb buffer gas cell. In particular, we investigated the case when pulses are highly elliptical (maximum relative optical power of σ^- component is only 15%), since several slow and stored light experiments typically use this level of ellipticity [4, 39]. We explore the effects of Ramsey sequences by comparing the behavior of EIT during the preparatory and the probe pulse by varying the length of the dark time between them. The Zeeman EIT resonances are then expected to exhibit the oscillation of transmission in magnetic field caused by Larmor precession during the dark time. The motivation of this work was in part to investigate the properties of the foreseen Ramsey oscillation with respect to pulse intensities and Rb density. Experimentally observed developments of the Zeeman EIT are compared with corresponding theoretical results. Our theoretical model based on time dependent Maxwell–Bloch equations qualitatively reproduces experimental observations. We are not aware of previous publications that show the time evolution of Zeeman EIT and Ramsey effect on this evolution when fast developing pulse propagates through Rb cell with buffer gas.

The detection of Raman–Ramsey oscillations on EIT line shapes presented in this work can find application in high precision magnetic field measurements and in determining the atomic decoherence rates.

2. Theory

2.1. Description of the model

The evolution of Rb atoms contained in a buffer-gas cell is calculated using time dependent optical Bloch equations for Rb density matrix $\hat{\rho}$

$$\frac{\partial \hat{\rho}}{\partial t} = D\nabla^2\hat{\rho} - \frac{\mathrm{i}}{\hbar}\Big[\hat{H}_{\mathrm{atom}}(B) + \hat{V}_{\mathrm{int}}(r,t), \hat{\rho}\Big] + \left(\frac{\partial \hat{\rho}}{\partial t}\right)_{\mathrm{SE}} + \left(\frac{\partial \hat{\rho}}{\partial t}\right)_{\mathrm{coll}}, \quad (1)$$

where $\hat{H}_{\mathrm{atom}}(B)$ is the atomic Hamiltonian in the external longitudinal magnetic field, $\hat{V}_{\mathrm{int}}(r,t)$ describes laser-atom interaction and the term with subscript SE corresponds to spontaneous emission. The hyperfine levels either coupled to the laser light or populated due to spontaneous emission are shown in the energy level diagram in figure 1.

Collisions with the buffer-gas affect the atomic evolution in several ways. First, Rb atoms acquire diffusive motion within the cell, as described by the first term at the right-hand

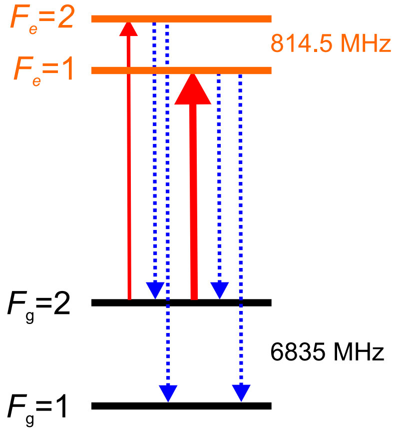

Figure 1. Energy level diagram for D_1 line transitions considered in the theoretical model. Solid lines represent transitions induced by the laser, while dotted lines correspond to possible spontaneous emission channels from excited levels. Frequency differences between adjacent hyperfine levels are shown.

side of (1) with D as the diffusion coefficient. Second, within each excited state manifold the populations of Zeeman sublevels are equalized, while the coherences are destroyed due to total collisional depolarization of the excited state [40, 41]. The collisions with the buffer gas also broaden the optical transition and together with the Rb–Rb collisions lead to the relaxation of the ground state populations and coherences. These effects correspond to the last term at the right-hand side of (1). For the buffer gas pressure of 30 Torr the collisional broadening of ≈300–400 MHz is comparable with the Doppler width, so that we use the approximation of the motionless atoms in the direction of the laser beam propagation. Detailed exposition of the theoretical model is given in [42]. The present experimental configuration requires some additions concerning time dependent features. Contrary to the steady state calculations in [42], here we are solving (1) in cylindrical coordinates (r, z) and *in time*. The effects of propagation of slowly varying envelopes (SVEs) of the laser electric field $\mathcal{E}$ and the polarization $\mathcal{P}$ of the Rb vapour are also incorporated via

$$\frac{1}{c}\frac{\partial \boldsymbol{\mathcal{E}}(r, z, t; B)}{\partial t} + \frac{\partial \boldsymbol{\mathcal{E}}(r, z, t; B)}{\partial z} = \frac{\mathrm{i}\omega}{2\epsilon_0 c}\boldsymbol{\mathcal{P}}(r, z, t; B), \quad (2)$$

where ϵ_0 is the vacuum dielectric constant, c is vacuum speed of light and ω is the laser frequency. The time dependence of these SVEs originates from the time dependent boundary condition for the electric field at the entrance to the Rb cell $\mathcal{E}(r, z = 0, t; B) = \mathcal{E}_{\mathrm{in}}(r, t)$. In the frequency domain the propagation equation is

$$\mathrm{i}\frac{\nu}{c}\boldsymbol{\mathcal{E}}(r, z, \nu; B) + \frac{\partial \boldsymbol{\mathcal{E}}(r, z, \nu; B)}{\partial z} = \frac{\mathrm{i}\omega}{2\epsilon_0 c}\boldsymbol{\mathcal{P}}(r, z, \nu; B). \quad (3)$$

The frequencies for which $\mathcal{E}_{\mathrm{in}}(r, \nu)$ is significant satisfy

$$\left|\frac{\nu}{c}\boldsymbol{\mathcal{E}}(r, z, \nu; B)\right| \ll \left|\frac{\partial \boldsymbol{\mathcal{E}}(r, z, \nu; B)}{\partial z}\right| \sim \left|\frac{\mathcal{E}_{\mathrm{in}}(r, \nu)}{L}\right|, \quad (4)$$

where L is the cell length, so that we can safely drop the first term from (2). This leads to

$$\frac{\partial \boldsymbol{\mathcal{E}}(r, z, t; B)}{\partial z} = \frac{\mathrm{i}\omega}{2\epsilon_0 c}\boldsymbol{\mathcal{P}}(r, z, t; B), \quad (5)$$

which is used, in conjunction with (1), for calculation of the transmitted electric field at $z = L$ and Zeeman EIT resonances at particular time instants. The normalized σ^- transmission corresponds to the ratio $I_{\mathrm{tr}}^-/I_{\mathrm{in}}^-$, where I_{tr}^- and I_{in}^- denote intensities of the σ^- component of a laser beam, after propagation through and before entering into the Rb cell, respectively. Numerical calculations are performed using the DOLFIN finite element library [43] (part of the FEniCS project [44]) and CBC.PDESys package [45].

2.2. Theoretical results

The EIT resonances were determined from calculated σ^- transmissions at a given time instant after the σ^- pulse is launched into the Rb cell, at various magnetic fields. The cell temperature is 67 °C. The period between the two pulses, when the laser beam was turned off, was set to 60 μs. Overall laser intensities during the first (preparatory) and the second (probe) pulse were 4.9 and 0.9 mW cm^{-2}, respectively. Both pulses were elliptically polarized with 15% of photons carrying the σ^- polarization. Calculated EIT curves at t = 6, 16, 100, and 328 μs from the beginning of the probe pulse are shown in figures 2(a)–(d), respectively.

From the calculated transmission signals, the amplitudes and the linewidths of Zeeman EIT resonances evolving in time were extracted and shown in figures 3(a) and (b), respectively. These results show that the central peak has higher amplitude and wider line shape soon after the start of the probe pulse.

3. Experiment

3.1. Description of the experiment

Propagation of the polarization laser pulses and temporal evolution of Zeeman EIT resonances are experimentally realized in the Hanle configuration. A schematic of the experiment is given in figure 4(a).

The external cavity diode laser is frequency locked to the hyperfine $F_g = 2 \to F_e = 1$ transition of the D_1 line in ^{87}Rb using the Doppler-free dichroic atomic vapour laser lock method [46, 47]. Gaussian profile for the laser beam is obtained by the short single mode optical fiber. In order to apply the Ramsey method of repeated interactions of a laser light with Rb atoms, the power of the first order diffracted beam from the AOM is modulated and transmitted through the cell. The linear polarization of the laser light is assured by the high quality polarizer. The Pockels cell and the λ/4 plate are used to generate laser pulses with elliptical polarization: pure σ^+ circular polarization is obtained when no voltage is applied to the cell, while 15% of the σ^- light is produced

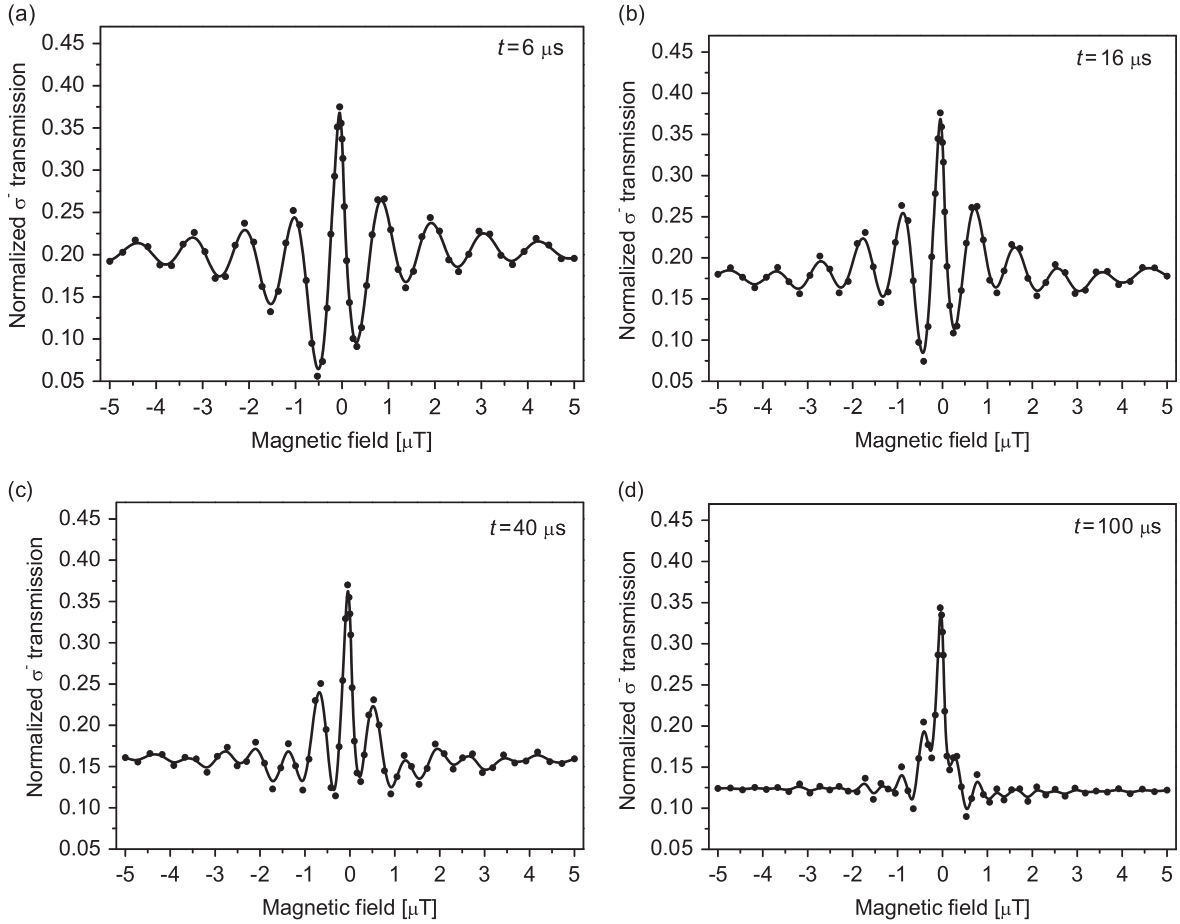

Figure 2. Time evolution of calculated Zeeman EIT resonances during the probe pulse with overall laser beam intensity of $I_2 = 0.9$ mW cm^{-2}. The overall laser beam intensity during the preparatory pulse is $I_1 = 4.9$ mW cm^{-2}. The dark period is $T_D = 60\,\mu$s. The resonances are reconstructed and normalized from σ^- transmission signals at four different times: (a) $t = 6\,\mu$s, (b) $t = 16\,\mu$s, (c) $t = 40\,\mu$s, and (d) $t = 100\,\mu$s. The cell temperature is 67 °C.

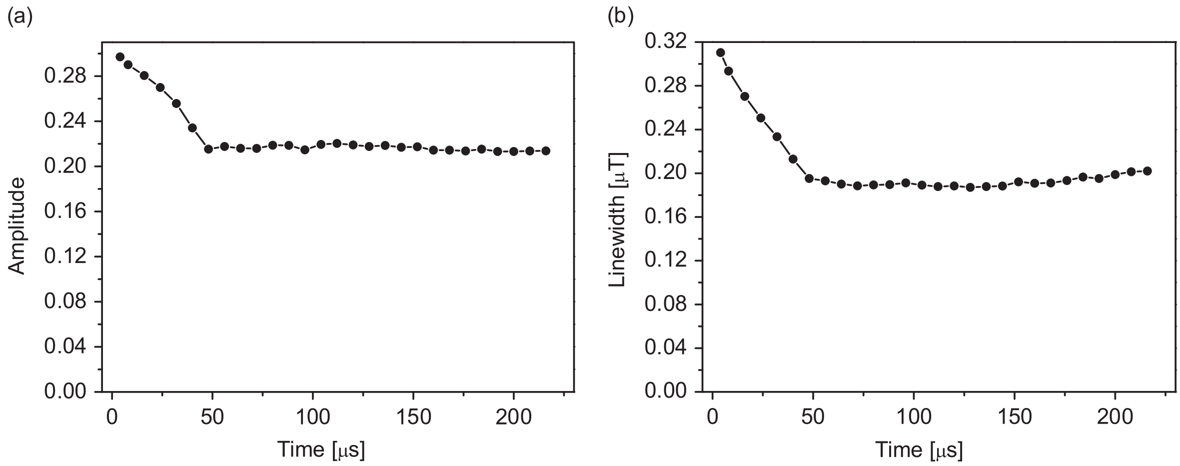

Figure 3. Theoretically obtained time evolution of Zeeman EIT (a) amplitudes and (b) linewidths of the central fringe during the probe pulse, for overall laser beam intensity of $I_2 = 0.9$ mW cm^{-2}. The overall laser beam intensity during the preparatory pulse is $I_1 = 4.9$ mW cm^{-2}. The dark period is $T_D = 60\,\mu$s. The cell temperature is 67 °C.

otherwise. The Rb cell containing 30 Torr of Ne buffer gas is 8 cm long and has 2.5 cm in diameter. The Rb cell was heated by using hot air circulating around the cell. Measurements were done at 67 °C and 85 °C. The Rb cell is shielded from stray magnetic fields by the triple μ-metal layers which reduce stray magnetic fields below 10 nT. In order to obey two-photon detuning, long solenoid placed around the Rb cell produces controllable longitudinal magnetic field in the range

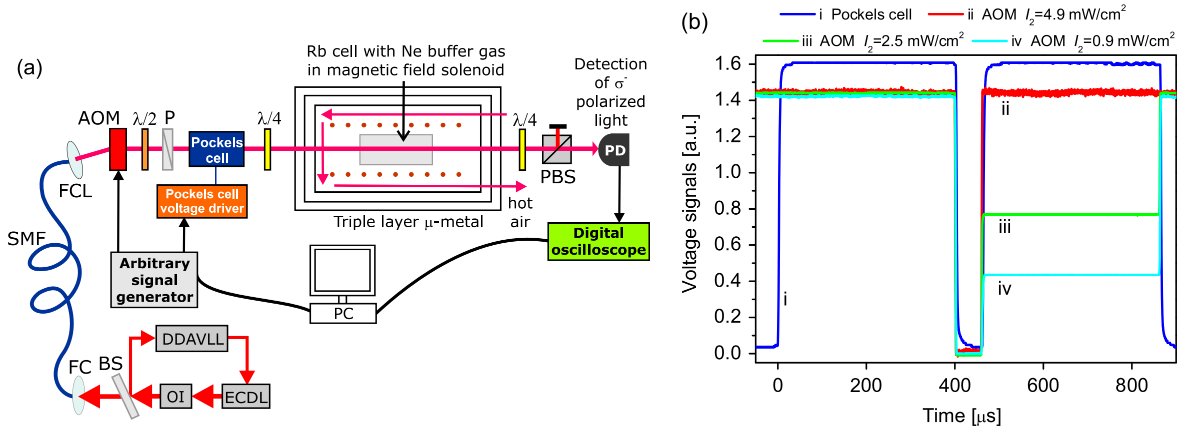

Figure 4. (a) Experimental setup: ECDL—external cavity diode laser; OI—optical insulator; DDAVLL—Doppler-free dichroic atomic vapour laser lock; BS—beam splitter; FC—fiber coupler; SMF—single-mode fiber; FCL—fiber collimator; AOM—acousto-optic modulator; P—polarizer; PBS—polarizing beam splitter; PD—photodetector. Hot air is used for heating the cell. (b) Pockels cell and AOM signals used in the experiment.

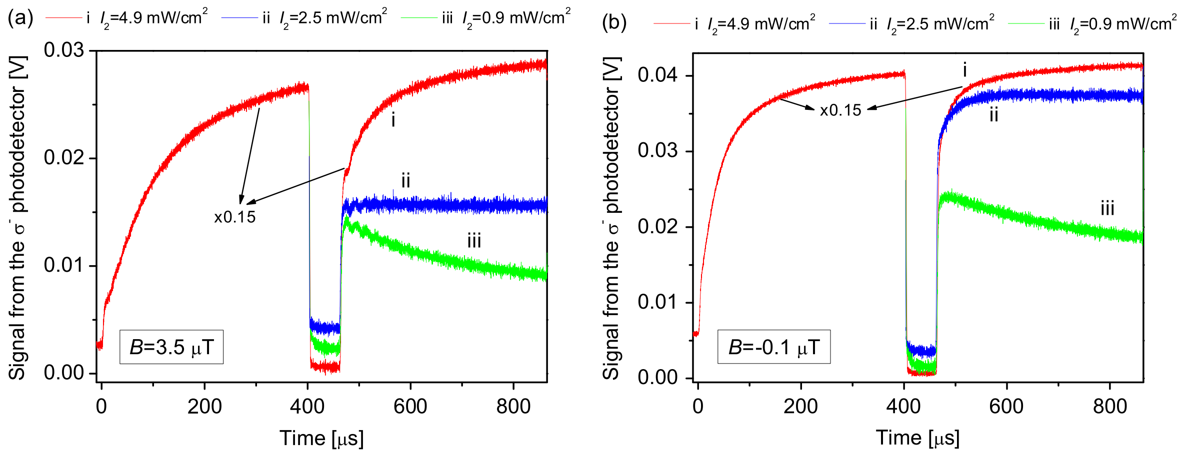

Figure 5. Measured σ^- transmission signals during preparatory and probe polarization laser pulse for magnetic field (a) 3.5 μT and (b) -0.1 μT. The curves in both figures correspond to the probe pulse overall intensity of (i) $I_2 = 4.9$ mW cm^{-2}, (ii) $I_2 = 2.5$ mW cm^{-2}, and (iii) $I_2 = 0.9$ mW cm^{-2}. The overall laser beam intensity during the preparatory pulse is $I_1 = 4.9$ mW cm^{-2}. The cell temperature is 67 °C.

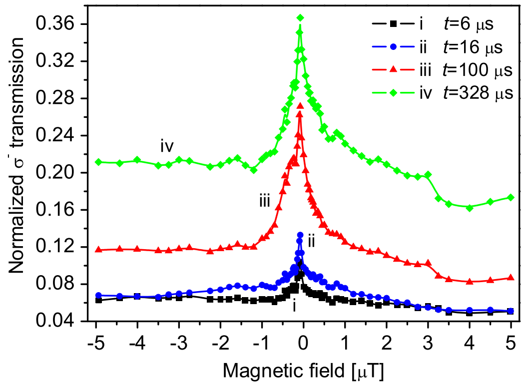

Figure 6. Time evolution of Zeeman EIT resonances during the preparatory pulse with overall laser beam intensity of $I_1 = 4.9$ mW cm^{-2}. The resonances are reconstructed and normalized from the σ^- transmission signals at four different times: $t = 6$ μs (curve i), $t = 16$ μs (curve ii), (c) $t = 100$ μs (curve iii), and (d) $t = 328$ μs (curve iv). The cell temperature is 67 °C.

of ± 10 μT. The σ^- light is extracted from the transmitted laser beam with the $\lambda/4$ plate and the PBS. Transmitted σ^- laser intensity over time, for a given magnetic field, is measured by the photodetector and recorded by the digital storage oscilloscope.

Laser pulses are produced after applying voltage pulses to the AOM and the Pockels cell as shown in figure 4(b). Note that the laser pulse here refers to the temporal change of a laser beam polarization. That is, polarization changes from σ^+ before the pulse, to elliptical polarization with 15% of σ^- relative optical power during the pulse. The first voltage pulse to the Pockels cell (signal (i)) is preparatory pulse that prepares Rb atoms into the dark state. Then, the voltages on the Pockels cell and the AOM are synchronously turned off for a certain period of dark time. During the dark time, Zeeman coherence makes a Larmor precession if the external magnetic field is not zero. After the dark time, the voltage pulses are again applied to AOM and Pockels cell and the second (probe) pulse, with the same polarization but intensity that can

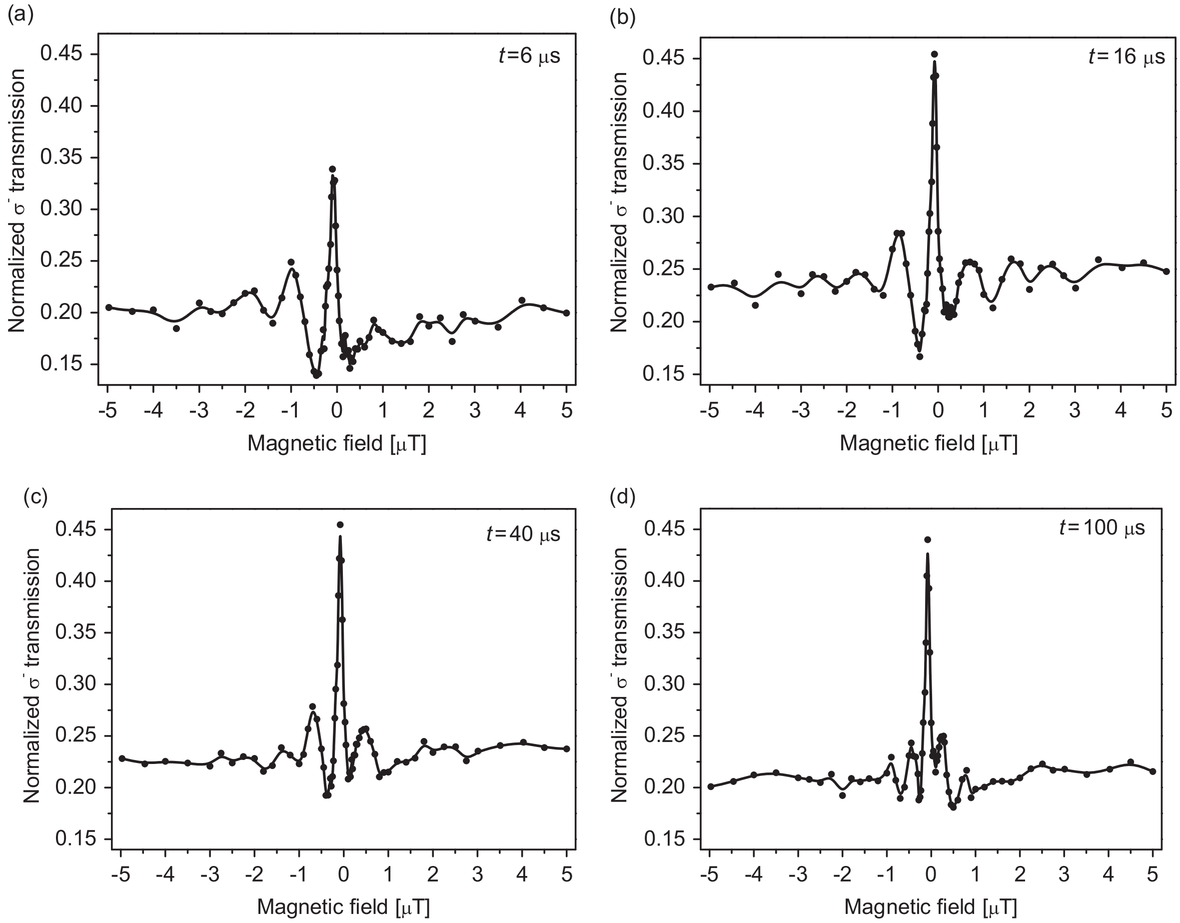

Figure 7. Time evolution of Zeeman EIT resonances during the probe pulse with overall laser beam intensity of I_2 = 0.9 mW cm^{-2}. The overall laser intensity during the preparatory pulse is I_1 = 4.9 mW cm^{-2}. The dark period is T_D = 60 μs. The resonances are reconstructed and normalized from the σ^- transmission signals at four different times (from top to bottom): t = 6 μs, t = 16 μs, t = 40 μs, and t = 100 μs. The cell temperature is 67 °C.

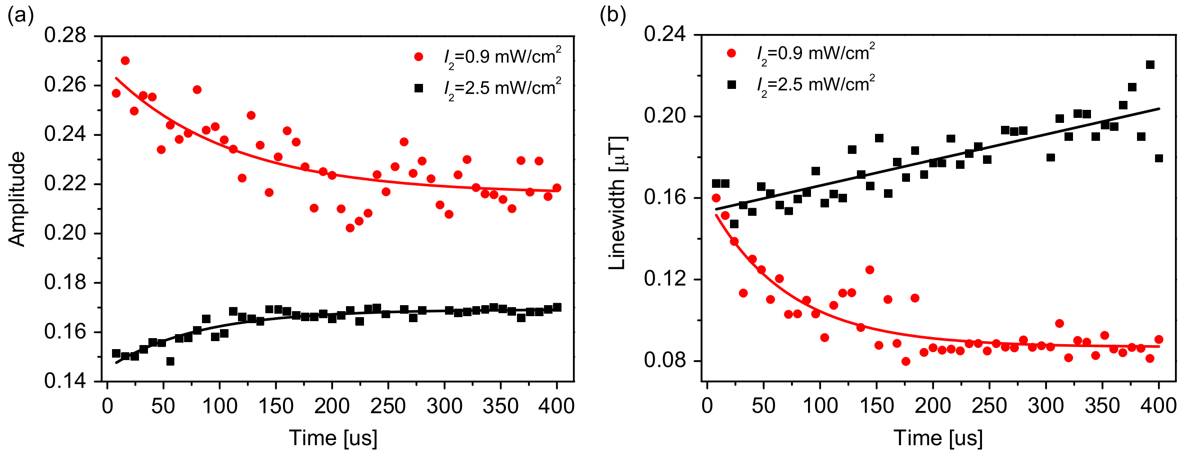

Figure 8. Experimentally obtained time evolution of Zeeman EIT (a) amplitude and (b) linewidth during the probe pulse. The overall intensities of the probe pulse are I_2 = 0.9 mW cm^{-2} or I_2 = 2.5 mW cm^{-2}. The overall laser intensity during the preparatory pulse is I_1 = 4.9 mW cm^{-2}. The dark period is T_D = 60 μs. The cell temperature is 67 °C. Solid lines are to guide the eye.

be different than the preparatory pulse, is created to probe the atomic coherences. At the end of the probe pulse, we return to a strong σ^+ polarization for several ms to repump atoms back to the Zeeman sublevels of the ground state before the next Ramsey sequence of pulses. Note that all the time we measure only the σ^- component of the elliptically polarized laser beam. We denote by I_1 and I_2 overall intensities of a laser beam during the preparatory (duration T_1) and probe pulse (duration T_2), respectively. Two synchronous voltage signals, controlling the AOM and the Pockels cell with fully

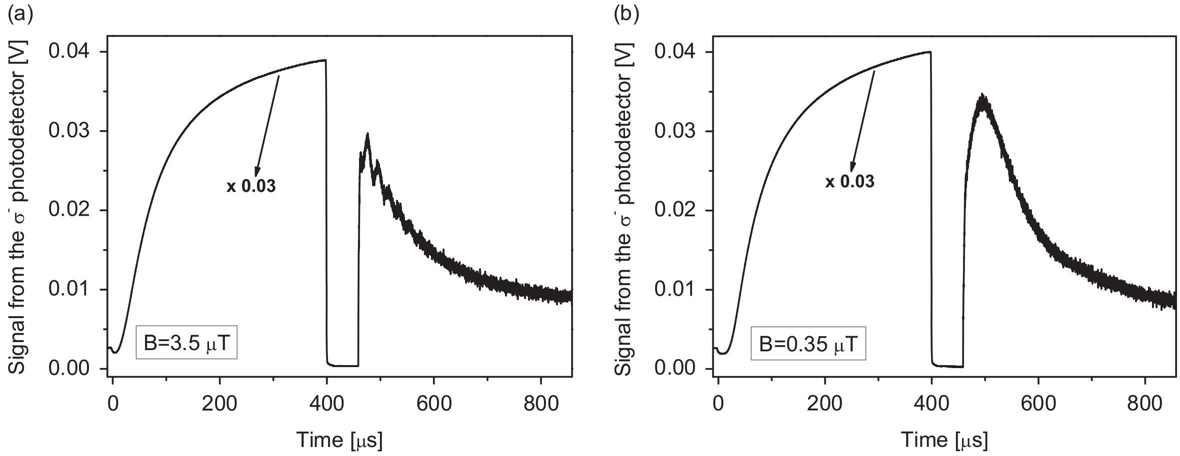

Figure 9. Measured σ^- transmission signals during preparatory and probe polarization laser pulse for magnetic field (a) 3.5 μT and (b) 0.35 μT. The curves in both figures correspond to the probe pulse overall intensity of I_2 = 4.8 mW cm^{-2}. The overall laser beam intensity during the preparatory pulse is I_1 = 49 mW cm^{-2}. The cell temperature is 85 °C.

adjustable amplitudes and durations, were generated by field-programmable gate array based signal generator and oscilloscope, as described in [48].

Development of Zeeman EIT for cell temperature of 67 °C, corresponding to Rb density of 5×10^{11} cm^{-3} [49], was measured with the following sequence of pulses: I_1 = 4.9 mW cm^{-2}, T_1 = 400 μs; T_D = 60 μs and T_D = 160 μs; T_2 = 400 μs. We varied the overall laser intensity during the probe pulse: I_2 = 4.9 mW cm^{-2} (AOM signal (ii)), I_2 = 2.5 mW cm^{-2} (AOM signal (iii)), and I_2 = 0.9 mW cm^{-2} (AOM signal (iv)) in order to measure the intensity dependencies of the: (1) σ^- transmission and (2) Zeeman EIT temporal development. The same Ramsey sequence was used for the cell temperature of 85 °C (Rb density of 1.4×10^{12} cm^{-3} [49]), except the higher laser intensity was required during the two pulses due to increased residual absorption: I_1 = 49 mW cm^{-2} and I_2 = 4.8 mW cm^{-2}.

3.2. Experimental results

In this section we show effects of the probe pulse intensity, the Ramsey sequences of successive excitation pulses, the external magnetic field and the cell temperature on propagation of pulses and development of EIT.

Measured transmissions of the σ^- component of a laser beam, during the preparatory and the probe pulse are shown in figure 5. The Rb cell temperature is 67 °C. Presented results are obtained for three values of the overall laser intensities during the probe pulse, and for the two values of magnetic field. The intensity and duration of the preparatory pulse are always I = 4.9 mW cm^{-2} and T_1 = 400 μs, so that during this pulse ^{87}Rb atoms are efficiently prepared into the dark state.

Transient behavior of the probe pulse depends on the laser intensity, duration of the dark time, and magnetic field. We show in figure 5 propagation of preparatory and probe pulse for two values of magnetic field, 3.5 and −0.1 μT, for three values of the probe pulse intensity, and for dark time of 60 μs. For the preparatory pulse intensity of 4.9 mW cm^{-2}, transmission of the probe pulse can be quite different depending on its intensity. At high intensity of the probe pulse (4.9 mW cm^{-2}), probe transmission increases with time due to optical pumping. When probe intensity is decreased to 2.5 mW cm^{-2}, transmission is constant in time. For the lowest probe intensity of 0.9 mW cm^{-2}, the probe pulse probes the coherences without significantly contributing to atomic evolution and optical pumping. The signal then decays due to decoherence and relaxation. At low magnetic field, the transmission of the probe is higher compared to transmission at higher magnetic fields (compare figures 5(a) and (b)), because more atoms are coherently prepared into the dark state by the preparatory pulse.

Due to Larmor precession of atomic polarization during the dark time, oscillations in the measured intensity of the probe pulse can be seen in figure 5(a), when intensity is low and magnetic field is different from zero. Frequency of observed fringes depends on the magnetic field, while their amplitudes depend on the amount of coherence between Zeeman sublevels. These results are in agreement with [35, 36]. The fringes on the transmission signal disappear when the σ^+ polarized laser beam is kept on between the preparatory and probe pulse (not shown), providing the evidence that observed fringes are indeed due to interference between coherently prepared atoms and the probe light.

From the transient curves of the σ^- transmission, like those in figure 5, taken at 70 different values of the longitudinal magnetic field, we have reconstructed Zeeman EIT resonances at different times during the development of preparatory and probe pulse. We first show Zeeman EIT resonances developing during the preparatory pulse (see curves (i)–(iv) in figure 6). As time progresses, EIT resonances keep the similar shape and only have higher amplitude since more atoms undergo dark state preparation.

Development of EIT during the probe pulse, when dark time is T_D = 60 μs is shown in figure 7. The overall laser beam intensities during the preparatory and the probe pulses were I_1 = 4.9 mW cm^{-2} and I_2 = 0.9 mW cm^{-2}. Characteristically, EIT resonance has central peak and fringes due to interference between atomic coherence precessing in the

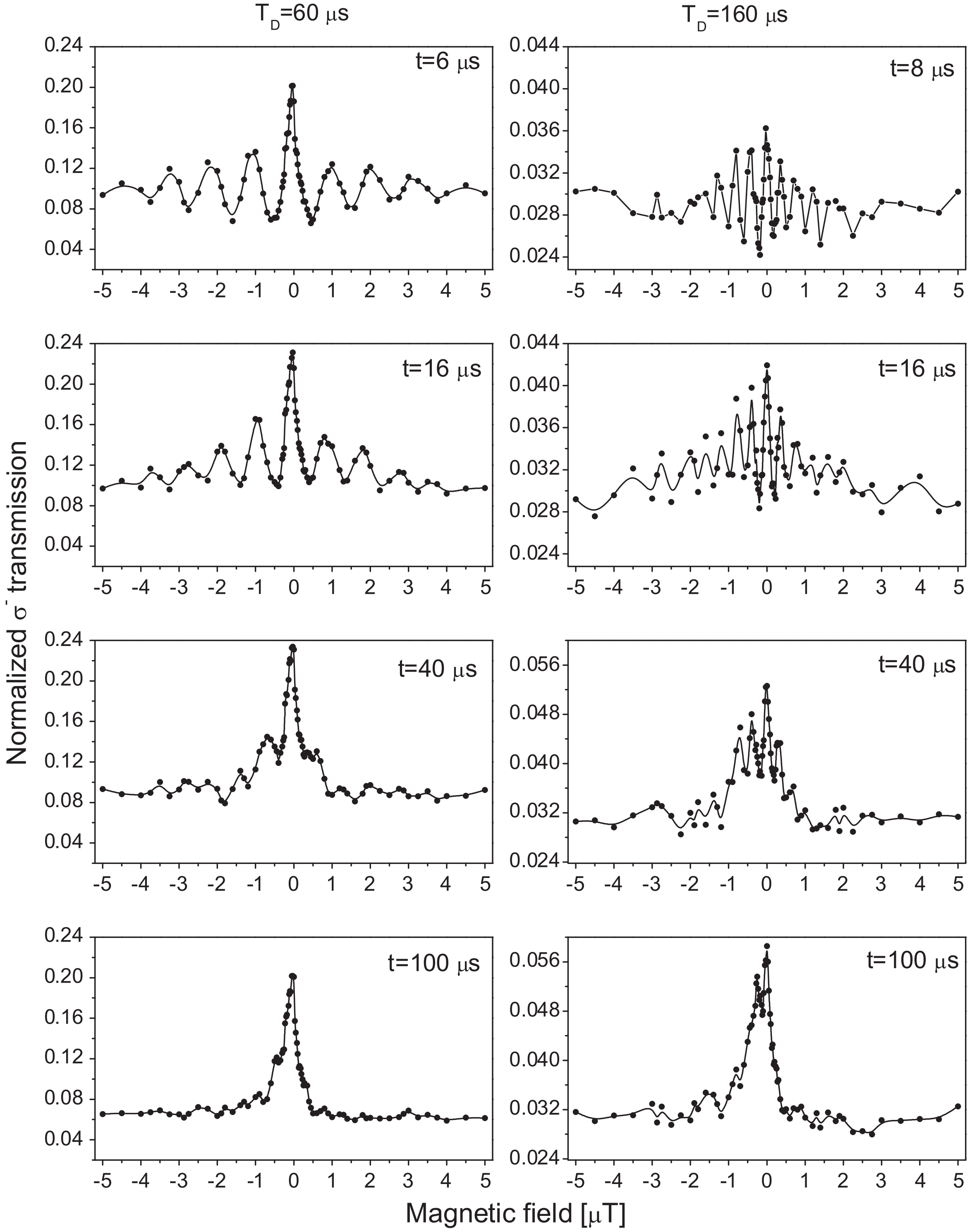

Figure 10. Time evolution of Zeeman EIT resonances during the probe pulse with overall laser beam intensity of I_2 = 4.8 mW cm^{-2}. The overall laser intensity during the preparatory pulse is I_1 = 49 mW cm^{-2}. The dark period is T_D = 60 μs (left column) and T_D = 160 μs (right column). The resonances are reconstructed and normalized from σ^- transmission signals at four different times (from top to bottom): t = 6 or 8 μs, t = 16 μs, t = 40 μs, and t = 100 μs. The cell temperature is 85 °C.

magnetic field and probe electric field (at t = 6 μs and t = 16 μs). The frequency width of the fringes decreases with time of precession. At about 40 μs since the beginning of the probe pulse only first order fringes are visible. At longer time they start merging with the central peak (t = 100 μs), and at even longer time only central peak remains. Experimental waveforms of EIT are in qualitative agreement with theoretical curves shown in figure 2, which are calculated under the same experimental conditions. We also found similar transition from EIT with fringes to EIT with only central peak at higher pulse intensity, except this transition is during shorter time.

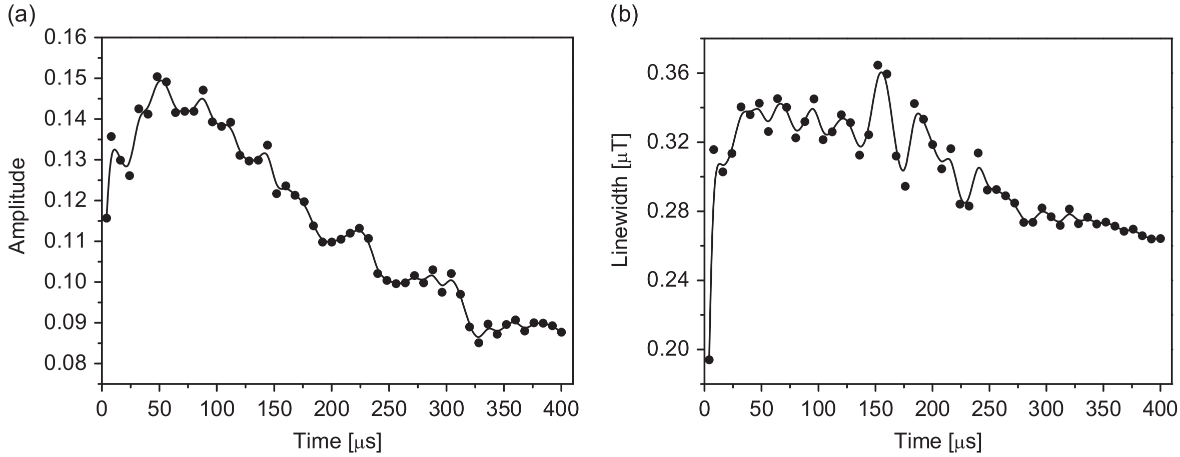

Figure 11. Experimentally obtained time evolution of Zeeman EIT (a) amplitude and (b) linewidth during the probe pulse. The overall intensities of the laser beam during preparatory and probe pulse are $I_1 = 49$ mW cm^{-2} and $I_2 = 4.8$ mW cm^{-2}, respectively. The dark period is $T_D = 60\,\mu$s. The cell temperature is 85 °C.

Time dependencies of Zeeman EIT amplitudes and linewidths are shown in figures 8(a) and (b), respectively, for dark time of 60 μs and two values of probe intensity, 0.9 and 2.5 mW cm^{-2}. One can see that more contrasted and narrower resonances are obtained when the probe pulse intensity is lower. Amplitudes of EIT behave differently at different pulse intensities. Similar to time dependence of transmitted probe intensity in figure 5, amplitudes of EIT resonances increase (decrease) with time for high (lower) probe intensity. When the pulse intensity is higher there is prevalent influence of power broadening. High intensity of the probe pulse also affects time evolution of Zeeman EIT. At high intensities (black squares at figure 8(b)) the strong electric field slows the precession, causing merging of the fringes with the central peak and broadening of the peak. However, at the beginning of the pulse, the EIT width is independent on the pulse intensity. It remains the same even when two pulses have very different intensities, as seen in figure 8. The significance of this finding is that EIT width will not vary with variations of intensities of the probe pulse as long as the pulse is shorter then a few μs. The width of the central peak is not sensitive to the intensity/power but to the absorbed energy of the laser light. The measured amplitudes agree well with calculated data shown in figure 3(a). However, the calculated linewidths (figure 3(b)) are somewhat larger than experimental ones.

In the investigation of the development of EIT when Raman detuning is achieved by modulating laser frequency at constant magnetic field, Yoshida *et al* have distinguished between the Raman–Ramsey and the hyperfine EIT spectra depending on the time gating within excitation pulse [34]. RRF were obtained at the pulse beginning while the EIT spectrum was obtained at its end. Due to variable magnetic field in our experiment, reconstructed σ^- transmission curve at each time instant consists of both Raman–Ramsey and EIT spectra.

Dependence of the transient development of Zeeman EIT resonances on Rb density and on the length of the dark time is studied by measuring signal pulse waveforms for Rb cell temperature of 85 °C and for two dark times: 60 μs and 160 μs. Similarly, σ^- transmission signal was measured at different magnetic fields during the preparatory and the probe pulse.

For investigations of transient behavior of EIT resonances, the intensities of preparatory and probe pulse were 49 and 4.8 mW cm^{-2}, respectively. At higher Rb density we needed to increase incident intensities in order to obtain signal from the transmitted σ^- component, that is high enough for good visibility of reconstructed EIT fringes. Measured transmissions of the σ^- component of the laser beam, during the preparatory and the probe pulse, are shown in figure 9 for two values of external magnetic field. As seen from figure 9(b), transmission of the σ^- component at very low magnetic field increases once the probe pulse has been established, and reaches the maximal value at some instant. After that moment, transmission starts to decay. This could be explained in terms that the probe pulse has enough optical power to further pump the atoms into the dark state, but at later times decoherence prevails and transmission drops. In the case of higher magnetic field, transmission drops right after the pulse is generated because of the higher value of two-photon detuning.

The reconstructed EIT curves for two dark times of 60 and 160 μs, are shown in figure 10.

RRF are observed at 6 and 8 μs after the beginning of the probe pulse. The fringes get narrower and weaker with precession time due to Zeeman decoherence, leading to a single EIT peak at later time instants. In classical Ramsey effect, the frequency width of the central Ramsey fringe is $1/(2 \cdot T_D)$. We have found that for dark times of 60 and 160 μs, the ratio of widths of the first order Ramsey fringes is in agreement with $1/(2 \cdot T_D)$ dependence. At these density and laser intensities fringes decay faster comparing to lower intensities (case with 67 °C cell temperature) because precession of the dark state is affected by electric field. The central peak is at each time instant also narrower when the dark time is 160 μs. Its narrowing could be explained by the work from [36] where authors have shown the increase of Zeeman decoherence rate because of the Rb–Rb spin-exchange collisions.

Measured time dependencies of EIT amplitudes and linewidths during the probe pulse when dark time is 60 μs and temperature is 85 °C are shown in figures 11(a) and (b), respectively. The amplitudes increase at the beginning of the probe pulse and decay later. This is in qualitative agreement with the σ^- transmission time dependence as presented in figure 9(b). The linewidths of EIT resonances are wider at higher density (85 °C versus 67 °C) due to the power broadening caused by higher laser beam intensity. At high pulse intensities needed for this Rb vapour density, the precession of the Zeeman coherences is slowed in the laser electric field and fringes start to merge with the central peak, thus broadening the resonance at earlier times.

4. Conclusion

We presented experimental and theoretical study of the transient response of EIT medium to propagation of laser polarization pulses resonant to EIT transition. Through observed time development of the σ^- pulse transmission at different magnetic fields, we reconstructed Zeeman EIT resonances corresponding to various time instants during pulse propagation. The EIT resonances during the probe pulse have characteristic Ramsey fringes at early times and a narrow central peak at later moments. Ramsey fringes or oscillations of probe transmission during pulse propagation in magnetic field are caused by Larmor precession during the dark time. The disappearance of fringes is faster for larger probe pulse intensities due to incoherent pumping and effects of electric field on precession of atomic coherences. The behavior of amplitudes and linewidths of the EIT central peak depends on the probe intensity and Rb density. At very low probe intensity they both monotonically decay if Rb density is low, while at higher density amplitudes and widths they first increase and then decay.

We have studied transients of the polarization laser pulses for the system that is often used in slow light and storage of light experiments. Thus, better knowledge of polarization pulse transmission and time development of EIT resonances is valuable.

Acknowledgments

We thank J Dimitrijević and Z D Grujić for fruitful and useful discussions. Authors acknowledge funding from Grants No. III45016 and OI171038 of the Ministry of Education, Science and Technological Development of the Republic of Serbia and Scopes JRP IZ7370_127942.

References

[1] Boller K J, Imamoğlu A and Harris S E 1991 *Phys. Rev. Lett.* **66** 2593
[2] Field J E, Hahn K H and Harris S E 1991 *Phys. Rev. Lett.* **67** 3062
[3] Arimondo E 1996 *Prog. Opt.* **35** 257
[4] Phillips D F, Fleischhauer A, Mair A, Walsworth D F and Lukin M D 2001 *Phys. Rev. Lett.* **86** 783
[5] Klein M J 2009 Slow and stored light in atomic vapor cells *PhD Thesis* Harvard University
[6] Fleischhauer M, Imamoğlu A and Marangos J P 2005 *Rev. Mod. Phys.* **77** 633
[7] Bai Y S, Mossberg T W, Lu N and Berman P R 1986 *Phys. Rev. Lett.* **57** 1692
[8] Fry E S, Li X, Nikonov D, Padmabandu G G, Scully M O, Smith A V, Tittel F K, Wang C, Wilkinson S R and Zhu S Y 1993 *Phys. Rev. Lett.* **70** 3235
[9] Greentree A D, Smith T B, Echaniz S R, Durrant A V, Marangos J P, Segal D M and Vaccaro J A 2002 *Phys. Rev.* A **65** 053802
[10] Harris S E and Luo Z-F 1995 *Phys. Rev.* A **52** R928
[11] Chen H X, Durrant A V, Marangos J P and Vaccaro J A 1998 *Phys. Rev.* A **58** 1545
[12] Park S J, Cho H, Kwon T Y and Lee H S 2004 *Phys. Rev. A* **69** 023806
[13] Wu Y and Yang X 2005 *Phys. Rev.* A **71** 053806
[14] Wu Y and Yang X 2004 *Phys. Rev.* A **70** 053818
[15] Meinert F, Basler C, Lambrecht A, Welte S and Helm H 2012 *Phys. Rev.* A **85** 013820
[16] Vanier J, Godone A and Levi F 1998 *Phys. Rev.* A **58** 2345
[17] Valente P, Failache H and Lezama A 2002 *Phys. Rev.* A **65** 023814
[18] Margalit L, Rosenbluh M and Wilson-Gordon A D 2012 *Phys. Rev.* A **85** 063809
[19] Margalit L, Rosenbluh M and Wilson-Gordon A D 2013 *Phys. Rev.* A **88** 023827
[20] Shwa D and Katz N 2014 *Phys. Rev.* A **90** 023858
[21] Valente P, Failache H and Lezama A 2003 *Phys. Rev.* A **67** 013806
[22] Berman P R and Salomaa R 1982 *Phys. Rev.* A **25** 2667
[23] Li Y Q and Xiao M 1995 *Opt. Lett.* **20** 1489
[24] Dimitrijević J, Arsenović D and Jelenković B M 2011 *New J. Phys.* **13** 033010
[25] Ramsey N F 1956 *Molecular Beams* (New York: Oxord University Press)
[26] Zanon T, Guérandel S, Clercq de E, Holleville D, Dimarcq N and Clairon A 2005 *Phys. Rev. Lett.* **94** 193002
[27] Zanon T, Trémine S, Guérandel S, Clercq de E, Holleville D, Dimarcq N and Clairon A 2005 *IEEE Trans. Instrum. Meas.* **54** 776
[28] Liu X, Mérolla J-M, Guérandel S, Clercq de E and Boudot R 2013 *Opt. Express* **21** 12451
[29] Chen X, Yang G-Q, Wang J and Zhan M-S 2010 *Chin. Phys. Lett.* **27** 113201
[30] Yisheng M, Jianliao D, Zhengfeng H, Huijuan H and Yuzhu W 2013 *Chin. Opt. Lett.* **11** 032701
[31] Supplee J M 2010 *J. Opt. Soc. Am.* B **27** 1543
[32] Chen J F, Lu W, Wang S, Loy M M T, Wong G K L and Du S 2010 *Opt. Lett.* **35** 1923
[33] Pati G S, Fatemi F K and Shahriar M S 2011 *Opt. Express* **19** 22388
[34] Yoshida I, Hayashi N, Fujita K, Taniguchi S, Hoshina Y and Mitsunaga M 2013 *Phys. Rev.* A **87** 023836
[35] Zibrov A S and Matsko A B 2001 *Phys. Rev.* A **65** 013814
[36] Shuker M, Firstenberg O, Sagi Y, Ben-kish A, Davidson N and Ron A 2008 *Phys. Rev.* A **78** 063818
[37] Braje D A, DeSavage S A, Adler C L, Davis J P and Narducci F A 2014 *J. Mod. Opt.* **61** 61
[38] Yang J, Tian Y, Tan B, Yun P and Gu S 2014 *J. Appl. Phys.* **115** 093109
[39] Mair A, Hager J, Phillips D F, Walsworth R L and Lukin M D 2002 *Phys. Rev.* A **65** 031802(R)

[40] Taichenachev A V, Yudin V I, Wynands R, Stahler M, Kitching J and Hollberg L 2003 *Phys. Rev.* A **67** 033810
[41] Failache H, Valente P, Ban G, Lorent V and Lezama A 2003 *Phys. Rev.* A **67** 043810
[42] Nikolić S N, Radonjić M, Krmpot A J, Lučić N M, Zlatković B V and Jelenković B M 2013 *J. Phys. B: At. Mol. Opt. Phys.* **46** 075501
[43] Anders L and Garth W 2010 *ACM Trans. Math. Softw.* **37** 20:1–20:28
[44] Logg A, Mardal K-A and Wells G N 2012 *Automated Solution of Differential equations by the Finite Element Method* (*Lecture Notes in Computational Science and Engineering* vol 84) (Berlin: Springer)
[45] Mortensen M, Langtangen H P and Wells G N 2011 *Adv. Water Resour.* **34** 1082
[46] Wasik G, Gawlik W, Zachorowski J and Zawadzki W 2002 *Appl. Phys.* B **75** 613
[47] Petelski T, Fattori M, Lamporesi G, Stuhler J and Tino G M 2003 *Eur. Phys. J.* D **22** 279
[48] Nikolić S N, Batić V, Panić B and Jelenković B M 2013 *Rev. Sci. Instrum.* **84** 063108
[49] Steck D A 2008 *Rubidium 87 D Line Data* (http://steck.us/alkalidata)